



Published in final edited form as:

*J Clin Neurophysiol*. 2017 November ; 34(6): 527–533. doi:10.1097/WNP.0000000000000411.

## Relationship Between Alpha Rhythm and the Default Mode Network: An EEG-fMRI Study

Anthony D. Bowman<sup>\*</sup>, Joseph C. Griffis<sup>†</sup>, Kristina M. Visscher<sup>‡</sup>, Allan C. Dobbins<sup>\*</sup>, Timothy J. Gawne<sup>§</sup>, Mark W. DiFrancesco<sup>||</sup>, Jerzy P. Szaflarski<sup>‡,¶</sup>

<sup>\*</sup>Department of Biomedical Engineering, University of Alabama at Birmingham, Birmingham, Alabama, U.S.A.

<sup>†</sup>Department of Psychology, University of Alabama at Birmingham, Birmingham, Alabama, U.S.A.

<sup>‡</sup>Department of Neurobiology, University of Alabama at Birmingham, Birmingham, Alabama, U.S.A.

<sup>§</sup>Department of Vision Sciences, University of Alabama at Birmingham, Birmingham, Alabama, U.S.A.

<sup>||</sup>Department of Radiology, Cincinnati Children's Hospital Medical Center, Cincinnati, Ohio, U.S.A.

<sup>¶</sup>Department of Neurology, University of Alabama at Birmingham, Birmingham, Alabama, U.S.A.

### Abstract

**Purpose:** Reports of the relationship between the default mode network (DMN) and alpha power are conflicting. Our goal was to assess this relationship by analyzing concurrently obtained EEG/functional MRI data using hypothesis-independent methods.

**Methods:** We collected functional MRI and EEG data during eyes-closed rest in 20 participants aged 19 to 37 (10 females) and performed independent component analysis on the functional MRI data and a Hamming-windowed fast Fourier transform on the EEG data. We correlated functional MRI fluctuations in the DMN with alpha power.

**Results:** Of the six independent components found to have significant relationships with alpha, four contained DMN-associated regions: One independent component was positively correlated with alpha power, whereas all others were negatively correlated. Furthermore, two independent components with opposite relationships with alpha had overlapping voxels in the medial prefrontal cortex and posterior cingulate cortex, suggesting that subpopulations of neurons within these classic nodes within the DMN may have different relationships to alpha power.

---

Address correspondence and reprint requests to Anthony D. Bowman, University of Alabama at Birmingham Epilepsy Center, 312 Civitan International Research Center, 1719 6th Avenue South, Birmingham, AL 35294-0021, U.S.A.; anbowman@uab.edu.

All work pertaining to this study was performed at the University of Alabama at Birmingham, Birmingham, AL, U.S.A.

This work was part of the first author's Master's Thesis in the Department of Biomedical Engineering at the University of Alabama at Birmingham, Birmingham, AL, U.S.A.

Presented in part at the 2015 Annual Meeting of the American Academy of Neurology held at the Walter E. Washington Convention Center in Washington, DC from April 18 to 25, 2015.

The authors have no funding or conflicts of interest to disclose.

**Conclusions:** Different parts of the DMN exhibit divergent relationships to alpha power. Our results highlight the relationship between DMN activity and alpha power, indicating that networks, such as the DMN, may have subcomponents that exhibit different behaviors.

### Keywords

EEG/fMRI; Default mode network; Alpha power; Independent component analysis; Thalamus

Even when at rest, the brain is active and this activity follows reliable patterns that can be observed using functional imaging techniques, as well as neurophysiologic methods.<sup>1-3</sup> During functional MRI (fMRI), the blood oxygenation level–dependent (BOLD) signal in the brain is recorded over time. Synchronization of the low-frequency fluctuations of this signal between regions allows for the so-called “resting state” networks to be defined.<sup>4,5</sup> The default mode network (DMN) is one such resting state network, typically defined to include regions of the medial prefrontal cortex (MPFC), anterior cingulate cortex and posterior cingulate cortex (PCC), cuneus/precuneus, and temporoparietal junction/angular gyrus.<sup>6-8</sup> Hippocampi, parahippocampal gyri, and frontopolar cortex are sometimes included in the DMN as regions that are “loosely integrated” with the DMN because of their presence in some studies.<sup>9,10</sup> Activity in the typical DMN regions is known to increase during the resting state and decrease when a subject is performing a task.<sup>11-13</sup> Increased activations within this network are related to the processes of memorization and creating associations.<sup>6</sup> Increased activation of the DMN is thus typically linked to introspection or “internal mentation” and integration of thought processes.<sup>2,14</sup> However, although the fMRI measures that produced these results provide relatively fine spatial resolution in the millimeter range, the BOLD signal remains an indirect and slow measure of neural activity.

In contrast to fMRI, scalp EEG is a high temporal resolution measure of neural activity in the brain with a relatively poor spatial resolution.<sup>15</sup> EEG can measure oscillations of neural activity in the brain, which has been well documented.<sup>16</sup> One such waveform is the alpha rhythm: activity in the 8 to 13 Hz range typically recorded from posterior/occipital electrodes. These alpha oscillations have been observed to strengthen during rest, particularly when the subject’s eyes are closed<sup>16</sup> and are typically modulated by performing cognitive tasks, in particular, they are selectively suppressed during directed visual attention.<sup>3,17</sup> Current thinking suggests that alpha power indexes the degree of selective attention toward visual objects.<sup>18,19</sup> EEG is a temporally precise measure of neural activity, as it measures changes in electric fields, allowing for exploring neuronal firing patterns with high temporal resolution. However, limited spatial resolution and lack of direct access to the deep brain structures mean that localization of EEG sources may be difficult.<sup>20,21</sup>

The poor spatial resolution of the EEG can, to a certain degree, be handled by combining it with the high spatial resolution of fMRI. This method of combining EEG with fMRI (EEG/fMRI) in recent years has proven useful for examining the physiologic and pathophysiologic states of the brain.<sup>22-25</sup> Development of preprocessing tools to remove gradient and electrocardiogram artifacts from EEG data has allowed for continuous EEG data to be analyzed in conjunction with imaging data, further opening up research opportunities.<sup>26,27</sup>

Previous attempts to elucidate the relationship between DMN activity and alpha oscillations have produced mixed results. The discrepancies between studies are not necessarily contradictory because different methods and techniques may lead to different results and conclusions. Earlier studies have correlated EEG with the results of resting positron emission tomography<sup>28,29</sup> and EEG with resting fMRI (eyes open or eyes closed) at magnetic field strengths between 1.5 and 4 T.<sup>22,23,30,31</sup> All the above-mentioned studies conducted hypothesis-driven analyses to conclude that some brain regions e.g., the thalamus or occipital cortex exhibits positive or negative relationship with alpha power. We identified only a few studies that applied hypothesis-independent (data-driven) methods to analyze EEG/fMRI data to examine the contributions of alpha power to the BOLD signal changes in the DMN regions. Independent component analysis (ICA) is a data-driven method that can identify spatially distributed brain regions that act in concert. Independent component analysis makes no assumptions regarding the stimulus or brain response and does not require specification of the hemodynamic response function, providing an advantage over analytical approaches that require precise knowledge of the hemodynamic response function. Independent component analysis allows for identification of temporary connections as well as more stable connections and is thus particularly useful for analysis of resting state fMRI data.<sup>32-34</sup> One such ICA study identified two main resting state networks that were positively associated with EEG power in the alpha band—one corresponding to the DMN (bilateral parietal lobule, posterior cingulate and precuneus, and bilateral prefrontal cortices) and one related to self-referential mental activity (anterior cingulate, cerebellum, and hypothalamus). Because this study tested correlations with multiple EEG frequencies, the authors showed that one region may have relationships with more than one EEG frequency and that these relationships can be independent of one another.<sup>11</sup> Another ICA study did not identify any significant correlations with alpha power.<sup>35</sup> These studies demonstrate that significant questions remain concerning the relationship between the DMN and alpha power. Using ICA, a method without *a priori* assumptions, we aim to shed further light on the alpha–DMN relationship. To do so, fMRI and EEG data were obtained simultaneously; voxels of the DMN network were identified by ICA and cross-correlated with alpha frequency power extracted from the EEG. Although we expected to identify several components corresponding to the DMN, we hypothesized that only some of them, especially thalami and occipital cortices, would correlate with alpha power.

## METHODS

### Subjects

Twenty healthy adult subjects (10 women and 10 men; aged 19–37) participated in this EEG/fMRI study after providing written informed consent. They were recruited from the general university population. Although none reported taking psychoactive medications, subjects were not specifically screened for recent caffeine or over-the-counter medication intake. Study criteria required all subjects to be aged between 19 and 65 years, have a normal developmental history, with no neurologic conditions, have completed at least a high school education, and have no contraindications to fMRI at 3 T. The study was approved by the Institutional Review Board at the University of Alabama at Birmingham. Each subject first underwent 10 minutes of resting state EEG collected outside the scanner room for

later comparison with data collected inside the scanner to confirm data quality. For each resting state period, subjects were instructed to keep their eyes closed, relax, and let their minds wander. Each subject underwent a T1-weighted anatomic scan and a resting state T2\*-weighted functional scan with simultaneous EEG recording (EEG/fMRI).

### MRI Acquisition and Preprocessing

The fMRI was performed on a Siemens Magnetom Allegra 3 T scanner. A T1-weighted structural image was collected (TR = 2,300 ms; voxel size of  $1.0 \times 1.0 \times 1.0$  mm; TE = 2.17 ms; FOV =  $25.6 \times 25.6 \times 19.2$  cm, matrix =  $256 \times 256 \times 192$  pixels with sagittal orientation) along with a T2\*-weighted functional scan (TR = 2 seconds; voxel size of  $3.8 \times 3.8 \times 4.0$  mm; TE = 30 ms; slice thickness = 4 mm; FOV =  $24 \times 24$  cm, matrix =  $60 \times 60$  with sagittal orientation; flip angle =  $70^\circ$ ) lasting for 10 minutes. The first two measurements (whole brain volumes) were excluded to allow for the scanner to achieve magnetic equilibrium, resulting in 298 measurements per scan. Each functional scan was then preprocessed with in-house MATLAB scripts using Statistical Parametric Mapping software (SPM12b, <http://www.fil.ion.ucl.ac.uk/spm/>) including slice timing and motion correction, normalization to the Montreal Neurological Institute template, and spatial smoothing using a Gaussian kernel (6-mm FWHM).

### EEG Acquisition and Preprocessing

EEG data were recorded across 64 channels at 2 kHz both before placing the subject inside the scanner as well as during the functional scan. Electrocardiographic data were also collected using two electrodes for later ballistocardiographic artifact removal. These data were collected continuously using an MR-compatible system (MagLink by Neuroscan, Inc., Charlotte, NC) with Curry 7 software. Timing of the start of every fMRI volume acquisition was recorded and inserted into the EEG data as events. Preprocessing using Curry 7 included band pass filtering between 1 and 35 Hz, constant baseline correction, removal of the echo-planar image artifact using a 15 sample rolling average of the echo-planar image gradient artifact aligned to the inserted events, and ballistocardiographic artifact suppression using the first three components from principal component analysis centered to the ballistocardiographic artifact on a per subject basis applied to the electrocardiographic channel.

### Image Processing

Independent component analysis of fMRI data results in segmentation of brain regions into maximally independent components (ICs), each consisting of a spatial map of activation and corresponding time course.<sup>36</sup> To quantify the reliability of each IC across multiple runs of ICA, the Infomax algorithm of ICASSO with a minimum cluster size of 50 was applied to the fMRI data.<sup>37</sup> Group-level ICA was performed using the Group ICA of fMRI Toolbox (GIFT; <http://mialab.mrn.org/software/gift/index.html>), first generating 22 group-level ICs followed by back generation of individual subject ICs. This IC generation was performed 50 times by ICASSO with the generated ICs then compared and grouped into maximally independent clusters. The stability index of each cluster was quantified by comparing intercluster and intracluster similarity as defined by Himberg et al.<sup>37</sup> with only those components with a stability index greater than 0.90 retained. Group-level ICs were

then visually screened and those consisting of mostly artifact (activation outside the brain, within ventricles, etc.) were excluded from further analyses. For optimal comparison with alpha power, we elected to decompose our own fMRI data as opposed to using networks defined based on a previously published database from a different group of participants.

### EEG Processing and Correlation

A time course of alpha power, with sampling coincident with imaging acquisition, was extracted from the original EEG data from four bipolar channels (P3-O1, P4-O2, P7-O1, and P8-O2) using a method similar to one previously described.<sup>22</sup> Each sample represented the mean power in the alpha frequency band of 8 to 13 Hz across the 4 bipolar channels using a Hamming-windowed fast Fourier transform spanning the corresponding imaging TR period of 2 seconds. After extraction, the resulting time course was convolved with the canonical hemodynamic response function as defined by SPM to better synchronize the temporal phase shifts of these EEG data and the BOLD data. This final alpha time course for each subject was correlated with the time course of each IC. The raw correlation coefficients were transformed into Fisher Z-scores and a one sample *t* test performed on the set of Z-scores for each IC. Multiple comparison correction using the false discovery rate method was then applied to the *P* values obtained from each *t* test.<sup>38</sup>

## RESULTS

EEG-fMRI data from 17 subjects were analyzed. Three of the original 20 subjects were excluded: Two had insufficient data because of premature removal from the scanner and one because of an incidental finding. An example of an IC time course and alpha power signal from one participant is shown in Fig. 1, demonstrating the correlation between this alpha power signal and the BOLD response from the IC. Group-level ICA produced 22 ICs, all with stability indices above 0.90. Six of these ICs were found to have significant correlations to alpha ( $P < 0.05$ ; Table 1), and four contained brain regions previously associated with the DMN (Fig. 2).

The other two ICs with significant correlations to alpha power included one component that comprised mainly of voxels in the cerebellum (IC10) and brain stem, whereas the majority of the voxels in the other component were within the right frontal and right temporal lobes (IC4, Fig. 3).

The four components shown in Fig. 2 are consistent with DMN networks obtained in other fMRI studies using ICA.<sup>39,40</sup> More specifically, the division of activation within parietal and posterior cingulate cortices and activation in the MPFC into separate ICs found in this study mirrors the results shown in the study by Allen et al.<sup>39</sup> The components identified include voxels in the typical midline structures (MPFC, PCC, and thalamus in IC5, IC8, IC11, and IC22) as well as lateral structures (posterior temporal, inferior parietal cortex in IC5 and IC22).

Of the 22 components identified with ICA, 16 were found to be not significantly correlated with alpha. These components include a deep occipital component, a more superficial occipital component, a bilateral component with voxels comprising the majority of both

temporal lobes, a component including bilateral parietal lobes, a component with bilateral temporal activations with a cluster in the MPFC, and a component with bilateral superior temporal activations. The other 10 components not listed were excluded from analysis after visual inspection showed activations either primarily in the ventricles, external to the brain, or consistent with movement artifact.

## DISCUSSION

Applying ICA to EEG/fMRI data allows for hypothesis-free identification of DMN components that correlate with alpha power and for identification of sources within the same DMN region that may have different behavior and possibly opposite relationships to alpha power (Fig. 4). This provides a key insight when considered in the context of DMN subnetworks and how the DMN relates to other brain networks.

Among the DMN networks identified in our study, all statistically significant correlations with alpha power were negative, with the exception of IC11. In that component, which comprises voxels primarily in the PCC and MPFC, BOLD signal changes were positively correlated with alpha ( $P = 0.0052$ ). These regions are thought to participate in internal adaptive processes of retrieval, representation, and direct manipulation of various working memory processes including organization, planning, and problem solving.<sup>41</sup> The positive correlation of these anterior DMN nodes (IC11) with alpha is also consistent with the “internal mentation” hypothesis or introspection theory of alpha power.<sup>14</sup> We observed a strong spatial overlap between IC5 and IC11, as shown in Fig. 4, indicating that these two components, despite their different relationships to alpha power, involve overlapping tissues.

The DMN is observed to be preferentially active during resting state and in the absence of performing a task.<sup>42</sup> During resting state, the DMN is theorized to play a role in introspection, mind wandering, or day dreaming the “introspection” hypothesis,<sup>14</sup> but is also theorized to assist in maintaining a level of outward vigilance, monitoring the environment for any stimuli that may require more direct, focused attention the “sentinel” hypothesis.<sup>42,43</sup> The diagram on the right side of Fig. 5 illustrates a model where, during rest, the neural system toggles between “sentinel” and “introspection” states. The DMN is hypothesized to contribute to each of these states and to shifting between them.

Given that the literature has ascribed a dual function to the DMN, it is reasonable to look for duality in the behavior of DMN regions. One duality to consider is the relationship to alpha power. To reiterate, high alpha power is thought to relate to suppression of attention to the external environment and to be actively modulated to suppress potentially distracting sensory information.<sup>18,19</sup> Suppression of sensory information is essential for introspection, in order that sensory information does not interfere with introspective information processing. Thus, components of the DMN associated with introspection are expected to be positively correlated with alpha power. Indeed, a set of DMN regions that are linked to introspection (the more ventromedial regions in IC11) were positively correlated with alpha power.<sup>44</sup> Furthermore, the posterior cingulate/precuneus, a prominent node of the DMN, has been suggested to function in part to suppress sensory information processing,<sup>6</sup>



and this region was also included in the component (IC11) that was positively correlated with alpha power.

Conversely, the proposed “sentinel” function of the DMN requires maintaining a level of outward vigilance and taking in sensory information. Brain regions with such a sentinel function would be expected to show negative relationships to alpha power. ICs 5, 22, and 8 showed a negative relationship to alpha power, consistent with a sentinel function. As can be seen in Fig. 4, these networks overlap with the proposed “introspection” network of IC11 but do encompass other regions. These results, showing spatially overlapping components that have both positive and negative relationships to alpha power, highlight the DMN’s functional duality and confirm that tissue within the same voxels can support distinct functional roles. Furthermore, the regions of strongest overlap (white areas in Fig. 4, including MPFC and PCC) may be key locations involved in integrating or switching between the DMN’s introspective and sentinel functions.

This switching between internal and external locus of attention is essential to regulating our conscious experience.<sup>8</sup> Pathology affecting the DMN, in particular the MPFC and PCC, would then be expected to have negative implications for attention, spontaneous thought, and consciousness. Such a link has been found between a disruption in PCC activity and disorders of consciousness when compared with healthy controls.<sup>45</sup> Deactivations in regions of the DMN, particularly the PCC, have also been found after spike-and-wave discharges in patients with idiopathic generalized epilepsy, accompanied by altered or loss of consciousness.<sup>46</sup> Previous work has also shown decreased cerebral blood flow to DMN regions in patients with impaired consciousness during generalized tonic–clonic seizures.<sup>47</sup> In this context, decreased activity in the overlapping regions of IC5 and IC11 (MPFC and PCC) may then be interpreted as an interruption of the sentinel and introspective modes of the DMN, resulting in the observed states of altered consciousness. This may imply an internal “push–pull” relationship to the modes of the DMN in addition to that put forth in the “network inhibition hypothesis” between the DMN and subcortical structures.<sup>48</sup>

To conclude, we have shown, using group ICA applied to fMRI, that the DMN can be decomposed into independent subnetworks. These subnetworks are partially overlapping and have both positive and negative correlations with EEG-recorded alpha power. The fact that the DMN can be decomposed into subnetworks with differing correlations with EEG alpha power may explain much of the inconsistency in previous studies looking to examine the link between the DMN and alpha power. The MPFC and the PCC are sites of overlap of two subnetworks that have opposite correlations with EEG alpha power, indicating their different proposed functions (sentinel vs. introspection). These data also suggest that the regions of overlap of networks may be involved in switching between introspection and sentinel functions.

## Acknowledgments

This work was supported through the UAB Epilepsy Center funds.

## REFERENCES

1. Arieli AM, Shoham DO, Hildesheim RI, Grinvald AM. Coherent spatiotemporal patterns of ongoing activity revealed by real-time optical imaging coupled with single-unit recording in the cat visual cortex. *J Neurophysiol*1995;73:2072–2093. [PubMed: 7623099]
2. Kay BP, Meng X, Difrancesco MW, Holland SK, Szaflarski JP. Moderating effects of music on resting state networks. *Brain Res*2012;1447:53–64. [PubMed: 22365746]
3. Knyazev GG, Slobodskoj-Plusnin JY, Bocharov AV, Pylkova LV. The default mode network and EEG alpha oscillations: an independent component analysis. *Brain Res*2011;1402:67–79. [PubMed: 21683942]
4. Damoiseaux JS, Rombouts SA, Barkhof F, et al. Consistent resting-state networks across healthy subjects. *Proc Natl Acad Sci U S A*2006;103:13848–13853. [PubMed: 16945915]
5. Morgan VL, Gore JC, Szaflarski JP. Temporal clustering analysis: what does it tell us about the resting state of the brain? *Med Sci Monit*2008;14:CR345–CR352. [PubMed: 18591915]
6. Buckner RL, Andrews-Hanna JR, Schacter DL. The brain's default network: anatomy, function, and relevance to disease. *Ann N Y Acad Sci*2008;1124:1–38. [PubMed: 18400922]
7. Greicius MD, Supekar K, Menon V, Dougherty RF. Resting-state functional connectivity reflects structural connectivity in the default mode network. *Cereb Cortex*2009;19:72–78. [PubMed: 18403396]
8. Mantini D, Vanduffel W. Emerging roles of the brain's default network. *Neuroscientist*2013;19:76–87. [PubMed: 22785104]
9. Huijbers W, Pennartz CM, Cabeza R, Daselaar SM. The hippocampus is coupled with the default network during memory retrieval but not during memory encoding. *PLoS One*2011;6:e17463. [PubMed: 21494597]
10. Samann PG, Wehrle R, Hoehn D, et al. Development of the brain's default mode network from wakefulness to slow wave sleep. *Cereb Cortex*2011;21:2082–2093. [PubMed: 21330468]
11. Mantini D, Perrucci MG, Del Gratta C, Romani GL, Corbetta M. Electrophysiological signatures of resting state networks in the human brain. *Proc Natl Acad Sci U S A*2007;104:13170–13175. [PubMed: 17670949]
12. Shulman GL, Corbetta M, Buckner RL, et al. Common blood flow changes across visual tasks: I. Increases in subcortical structures and cerebellum but not in nonvisual cortex. *J Cogn Neurosci*1997;9:624–647. [PubMed: 23965121]
13. Shulman GL, Fiez JA, Corbetta M, et al. Common blood flow changes across visual tasks: II. Decreases in cerebral cortex. *J Cogn Neurosci*1997;9:648–663. [PubMed: 23965122]
14. Mason MF, Norton MI, Van Horn JD, Wegner DM, Grafton ST, Macrae CN. Wandering minds: the default network and stimulus-independent thought. *Science*2007;315:393–395. [PubMed: 17234951]
15. Burle B, Spieser L, Roger C, Casini L, Hasbroucq T, Vidal F. Spatial and temporal resolutions of EEG: is it really black and white? A scalp current density view. *Int J Psychophysiol*2015;97:210–220. [PubMed: 25979156]
16. Berger H. Über das elektroencephalogramm des menschen. *Archiv für Psychiatrie und Nervenkrankheiten*1929;87:527.
17. Petsche H, Kaplan S, von Stein A, Filz O. The possible meaning of the upper and lower alpha frequency ranges for cognitive and creative tasks. *Int J Psychophysiol*1997;26:77–97. [PubMed: 9202996]
18. Foxe JJ, Snyder AC. The role of alpha-band brain oscillations as a sensory suppression mechanism during selective attention. *Front Psychol*2011;2:154. [PubMed: 21779269]
19. Payne L, Sekuler R. The importance of ignoring Alpha oscillations protect selectivity. *Curr Dir Psychol Sci*2014;23:171–177. [PubMed: 25530685]
20. Koles ZJ. Trends in EEG source localization. *Electroencephalogr Clin Neurophysiol*1998;106:127–137. [PubMed: 9741773]
21. Pascual-Marqui R. Review of methods for solving the EEG inverse problem. *Int J Bioelectromagnetism*1999;1:75–86.



22. DiFrancesco MW, Holland SK, Szaflarski JP. Simultaneous EEG/functional magnetic resonance imaging at 4 Tesla: correlates of brain activity to spontaneous alpha rhythm during relaxation. *J Clin Neurophysiol*2008;25:255–264. [PubMed: 18791470]
23. Goldman RI, Stern JM, Engel J Jr, Cohen MS. Simultaneous EEG and fMRI of the alpha rhythm. *Neuroreport*2002;13:2487–2492. [PubMed: 12499854]
24. Kobayashi E, Bagshaw AP, Grova C, Gotman J, Dubeau F. Grey matter heterotopia: what EEG-fMRI can tell us about epileptogenicity of neuronal migration disorders. *Brain*2006;129:366–374. [PubMed: 16339793]
25. Pittau F, Dubeau F, Gotman J. Contribution of EEG/fMRI to the definition of the epileptic focus. *Neurology*2012;78:1479–1487. [PubMed: 22539574]
26. Allen PJ, Josephs O, Turner R. A method for removing imaging artifact from continuous EEG recorded during functional MRI. *Neuroimage*2000;12:230–239. [PubMed: 10913328]
27. Stern JM. Simultaneous electroencephalography and functional magnetic resonance imaging applied to epilepsy. *Epilepsy Behav*2006;8:683–692. [PubMed: 16630747]
28. Sadato N, Nakamura S, Oohashi T, et al. Neural networks for generation and suppression of alpha rhythm: a PET study. *Neuroreport*1998;9:893–897. [PubMed: 9579686]
29. Schreckenberger M, Lange-Asschenfeld C, Lochmann M, et al. The thalamus as the generator and modulator of EEG alpha rhythm: a combined PET/EEG study with lorazepam challenge in humans. *Neuroimage*2004;22:637–644. [PubMed: 15193592]
30. Laufs H, Kleinschmidt A, Beyerle A, et al. EEG-correlated fMRI of human alpha activity. *Neuroimage*2003;19:1463–1476. [PubMed: 12948703]
31. Laufs H, Krakow K, Sterzer P, et al. Electroencephalographic signatures of attentional and cognitive default modes in spontaneous brain activity fluctuations at rest. *Proc Natl Acad Sci U S A*2003;100:11053–11058. [PubMed: 12958209]
32. Bartels A, Zeki S. The chronoarchitecture of the human brain—natural viewing conditions reveal a time-based anatomy of the brain. *Neuroimage*2004;22:419–433. [PubMed: 15110035]
33. Karunanayaka P, Schmithorst VJ, Vannest J, Szaflarski JP, Plante E, Holland SK. A group independent component analysis of covert verb generation in children: a functional magnetic resonance imaging study. *Neuroimage*2010;51:472–487. [PubMed: 20056150]
34. Kay BP, DiFrancesco MW, Privitera MD, Gotman J, Holland SK, Szaflarski JP. Reduced default mode network connectivity in treatment-resistant idiopathic generalized epilepsy. *Epilepsia*2013;54:461–470. [PubMed: 23293853]
35. Neuner I, Arrubla J, Felder J, Shah NJ. Simultaneous EEG-fMRI acquisition at low, high and ultra-high magnetic fields up to 9.4 T: perspectives and challenges. *Neuroimage*2013;102:71–79. [PubMed: 23796544]
36. Calhoun C, Adali T, Pearlson GD, Pekar J. A method for making group inferences from functional MRI data using independent component analysis. *Hum Brain Mapp*2001;14:140–151. [PubMed: 11559959]
37. Himberg J, Hyvarinen A, Esposito F. Validating the independent components of neuroimaging time series via clustering and visualization. *Neuroimage*2004;22:1214–1222. [PubMed: 15219593]
38. Benjamini Y, Hochberg Y. Controlling the false discovery rate: a practical and powerful approach to multiple testing. *J R Stat Soc Series B Stat Methodol*1995;57:289–300.
39. Allen EA, Erhardt EB, Damaraju E, et al. A baseline for the multivariate comparison of resting-state networks. *Front Syst Neurosci*2011;5:2. [PubMed: 21442040]
40. Heine L, Soddu A, Gomez F, et al. Resting state networks and consciousness: alterations of multiple resting state network connectivity in physiological, pharmacological, and pathological consciousness states. *Front Psychol*2012;3:295. [PubMed: 22969735]
41. Binder J, Frost J, Hammeke T, Bellgowan P, Rao S, Cox R. Conceptual processing during the conscious resting state: a functional MRI study. *J Cogn Sci*1999;11:80–93.
42. Raichle ME, MacLeod M, Snyder Z, Powers WJ, Gusnard D, Shulman GL. A default mode of brain function. *Proc Natl Acad Sci U S A*2001;98:676–682. [PubMed: 11209064]
43. Gilbert SJ, Dumontheil I, Simons JS, Frith CD, Burgess PW. Comment on “Wandering minds: the default network and stimulus-independent thought”. *Science*2007;317:43. Author reply. [PubMed: 17615325]

44. Gusnard DA, Akbudak E, Shulman GL, Raichle ME. Medial prefrontal cortex and self-referential mental activity: relation to a default mode of brain function. *Proc Natl Acad Sci U S A*2001;98:4259–4264. [PubMed: 11259662]
45. Crone JS, Schurz M, Holler Y, et al. Impaired consciousness is linked to changes in effective connectivity of the posterior cingulate cortex within the default mode network. *Neuroimage*2015;110:101–109. [PubMed: 25620493]
46. Gotman J, Grova C, Bagshaw A, Kobayashi E, Aghakhani Y, Dubeau F. Generalized epileptic discharges show thalamocortical activation and suspension of the default state of the brain. *Proc Natl Acad Sci U S A*2005;102:15236–15240. [PubMed: 16217042]
47. Blumenfeld H, Varghese GI, Purcaro MJ, et al. Cortical and subcortical networks in human secondarily generalized tonic–clonic seizures. *Brain*2009;132:999–1012. [PubMed: 19339252]
48. Danielson NB, Guo JN, Blumenfeld H. The default mode network and altered consciousness in epilepsy. *Behav Neurol*2011;24:55–65. [PubMed: 21447899]

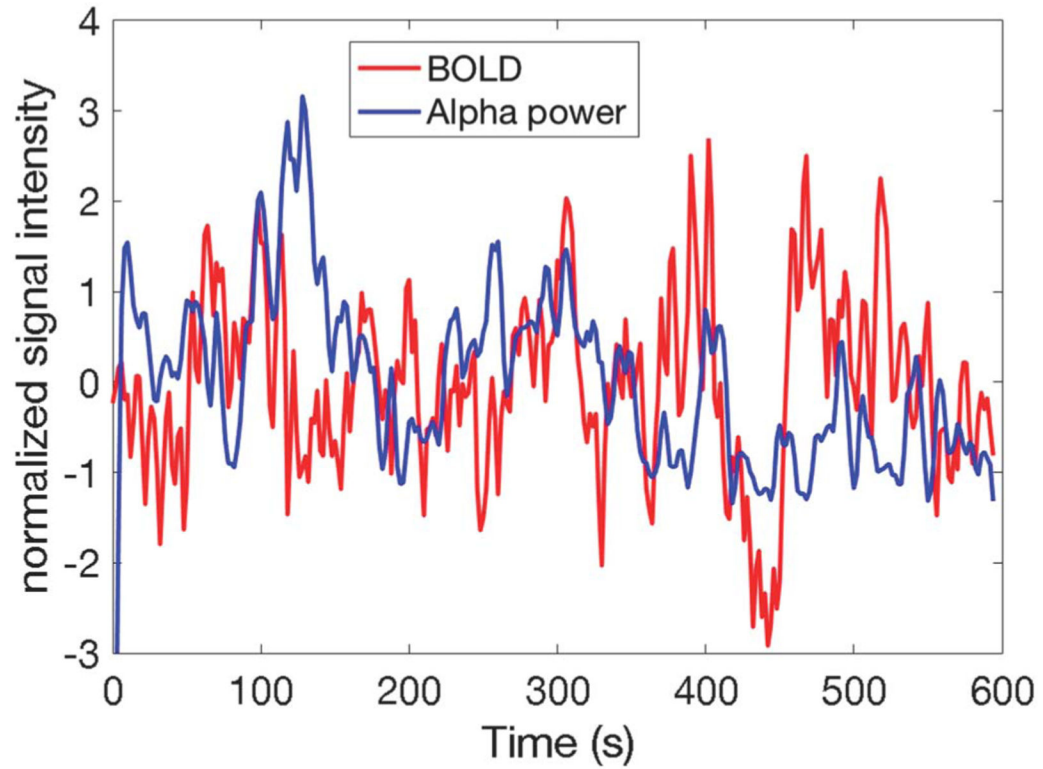


**FIG. 1.**

For illustration, we show a BOLD time course for IC11 in red for a representative participant. In blue is the alpha time course for the same participant's data. To fit these images to the same plot, both time courses are normalized by their SD. Note that the alpha time course represents alpha power averaged over a 2-second window and then convolved with a function to account for the hemodynamic delay. The resulting time course was used to identify the correlation between the BOLD signal and alpha oscillations. Also note that IC11 includes orbital and medial prefrontal regions coupled with posterior cingulate cortex. This was the only IC that exhibited a positive correlation with alpha power ( $P = 0.0192$ ). BOLD, blood oxygenation level-dependent; IC, independent component.

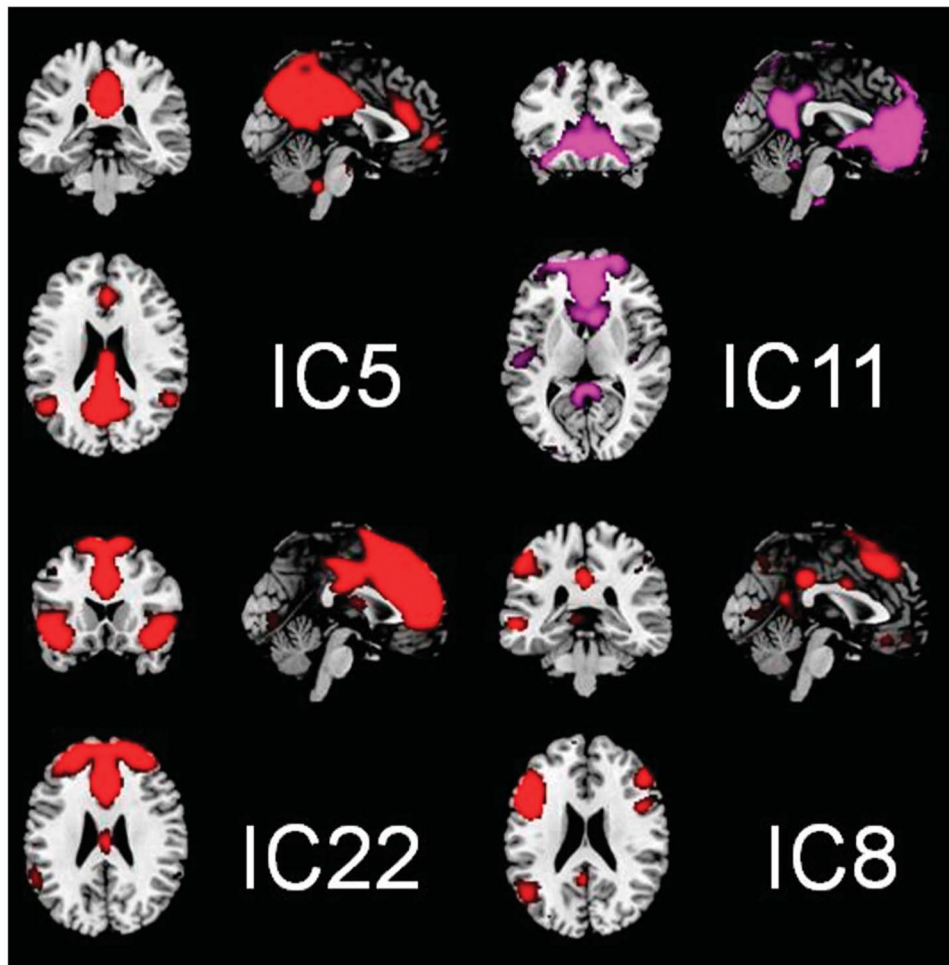


**FIG. 2.** Group-level ICs containing DMN regions significantly correlated with alpha. Negative correlations in red; positive correlations in violet. IC5: Posterior cingulate and parietal cortex, negative correlation ( $P = 0.0336$ ). IC11: Orbital and medial prefrontal regions coupled with posterior cingulate cortex, positive correlation ( $P = 0.0192$ ). IC22: Thalamus, medial frontal, and bilateral temporal activations, negative correlation ( $P = 0.0216$ ). IC8: Bilateral, lateral, and superior frontal and cingulate cortex, negative correlation ( $P = 0.0185$ ). DMN, default mode network; IC, independent component.

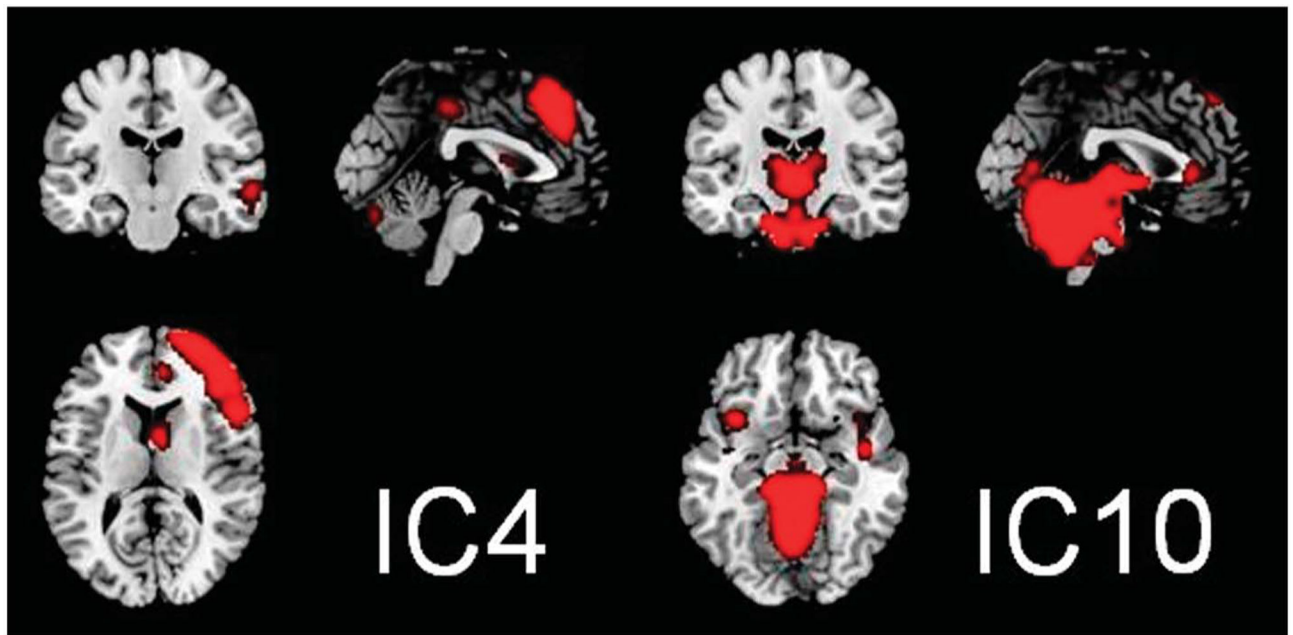


**FIG. 3.** Group-level ICs significantly correlated with alpha (non-DMN components). Negative correlations in red. IC4: Right frontal and right temporal regions ( $P=0.0195$ ). IC10: Cerebellum and brain stem ( $P=0.0084$ ). DMN, default mode network; IC, independent component.

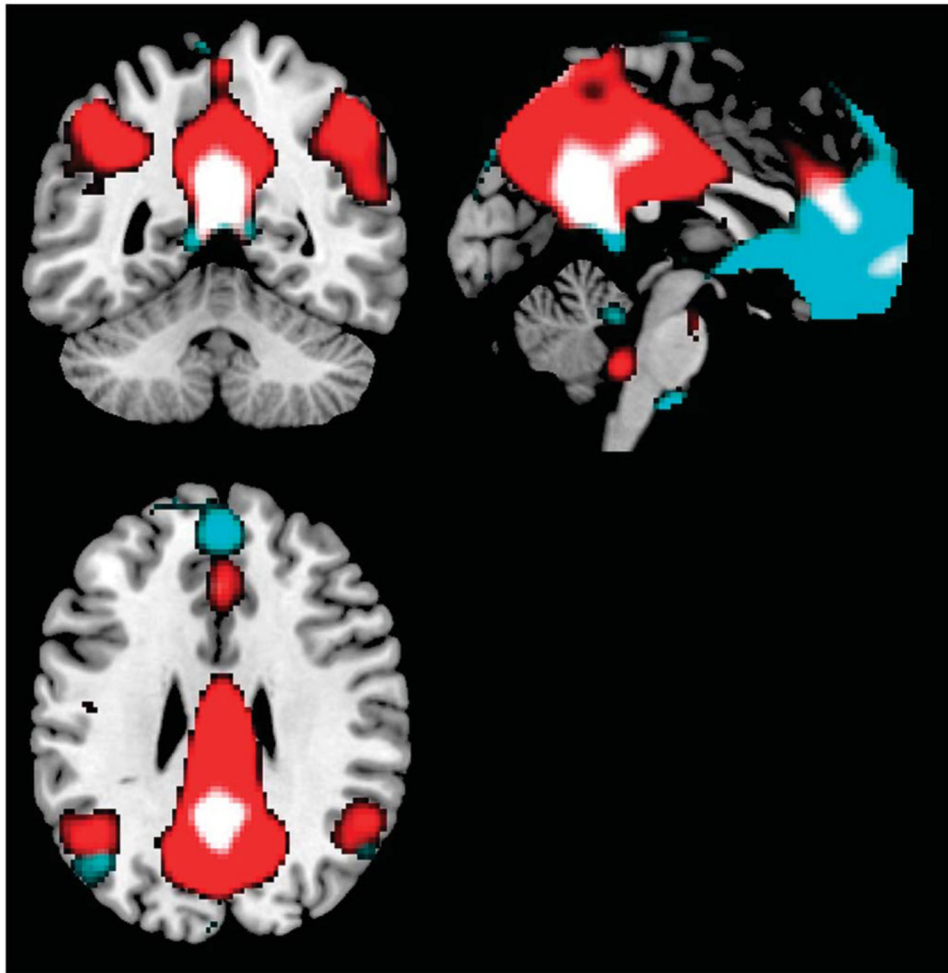


**FIG. 4.** Composite overlay showing overlap (white) of IC11 (cyan) and IC5 (red). IC, independent component.



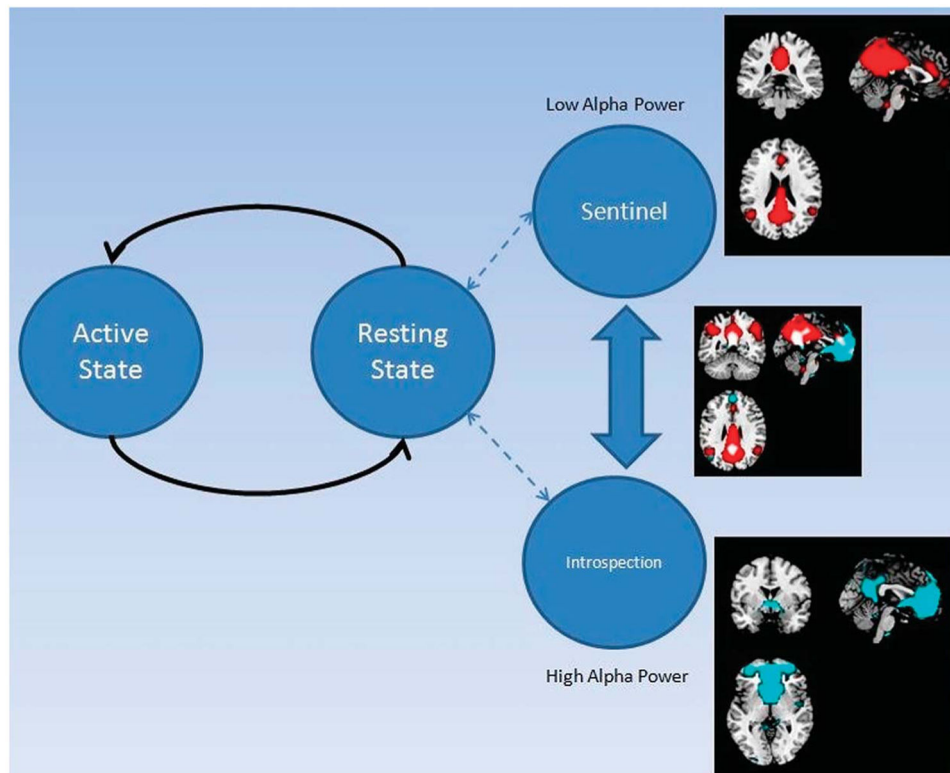


**FIG. 5.** Diagram showing DMN function toggling between sentinel and introspective states correlated with low and high alpha power. Associated ICs based on their correlation with alpha power are shown to the right, IC5 above, and IC11 below. DMN, default mode network; IC, independent component.

**TABLE 1.**  
All Independent Components of the BOLD Signal With a Significant Relationship to Alpha Power

IC	DMN?	Brain Region	Sign of Correlation With Alpha Power	P
IC4	Not DMN	Right frontal and right temporal cortex	Negative	0.02
IC5	DMN	Posterior cingulate and parietal cortex	Negative	0.03
IC8	DMN	Superior frontal and cingulate cortex	Negative	0.02
IC10	Not DMN	Cerebellum and brain stem	Negative	0.01
IC11	DMN	Orbital and medial prefrontal regions, posterior cingulate	Positive	0.02
IC22	DMN	Thalamus, medial frontal, and bilateral temporal	Negative	0.02

ICs are listed, followed by indication of whether the component was judged to be a part of the DMN, a rough description of the brain regions encompassed by the IC, the sign of the correlation with alpha power, and a *P* value of that effect.

BOLD, blood oxygenation level–dependent; DMN, default mode network; IC, independent component.